

Dynamics importance sampling for the activation problem in nonequilibrium continuous systems and maps

Stefano Beri^a, Riccardo Mannella^b, Peter V. E. McClintock^a

^aDepartment of Physics, Lancaster University LA1 4YB, Lancaster, United Kingdom;

^bDipartimento di Fisica, Università di Pisa Via Buonarroti 2, Pisa, Italy.

ABSTRACT

A numerical approach based on dynamic importance sampling (DIMS) is introduced to investigate the activation problem in two-dimensional nonequilibrium systems. DIMS accelerates the simulations and allows the investigation to access noise intensities that were previously forbidden. A shift in the position of the escape path compared to a heteroclinic trajectory calculated in the limit of zero noise intensity is directly observed. A theory to account for such shifts is presented and shown to agree with the simulations for a wide range of noise intensities.

Keywords: Non Linear Dynamics, Non Equilibrium Systems, Numerical Simulations

1. INTRODUCTION

The study of stochastic processes in nonlinear systems is a very wide and important subject within modern physics as they are one of the main ways to describe the dynamics of a real system subject to a source of “noise”. If the noise intensity is small, the system is expected to spend the majority of its time in the close vicinity of some stable equilibrium point. Nevertheless, very rarely, a large fluctuation may drive the system far from the stable state, and eventually settle it in the basin of attraction of a different stable structure. As a result of this *activation process*, the qualitative dynamics of the system may change dramatically. Consider for example a vertical cavity surface emitting laser (VCSEL) operating with two stable linearly polarised modes; the random fluctuations due to spontaneous emission in the active medium may induce strong changes in the polarization resolved light intensity.¹⁻⁴ In biological membranes, a current of ions passes through open ionic channels⁵ as the result of an activation process. Moreover, activation processes lie at the heart of many other physical phenomena in nonequilibrium systems, such as stochastic resonance,⁶ directed diffusion in stochastic ratchets.⁷⁻⁹ The Kramers activation process lies within this class of problems.¹⁰⁻¹² Despite its importance, the problem of activation cannot be regarded as solved. On the theoretical side, important steps toward the solution have been taken in the regime of zero noise intensity. It has been predicted that, even though the activation events become exponentially rare when the noise intensity approaches zero, they take place with increasing probability along activation trajectories that are close to an optimal trajectory. Such a *most probable escape path* (MPEP) can be obtained solving an auxiliary Hamiltonian system.¹³⁻²⁰ The same picture still applies even for escape at short times (i.e. before quasi-equilibrium has been established).²¹ The solution of the escape problem using the MPEP is in principle true only for the limit of zero noise intensity. However, for real systems, the intensity of noise fluctuations is necessarily finite. More recently it has been established²² that finite noise diffusion does more than just changing the prefactor of the exponential. It causes the system to follow a path that differs from the zero-noise theoretical MPEP.

During the last years, in particular due to the availability of fast computers, the activation problem has also been extensively studied numerically, in particular using Monte Carlo simulations. However, even for simple systems, the simulation time grows exponentially with decreasing noise intensity. Consequently, the really interesting range of noise intensities, i.e. small enough for valid comparisons to be made with theoretical predictions, have in practice been inaccessible to numerical experiments. Intensive efforts are therefore being made to find ways of speeding up the simulations.²³⁻²⁵ The probability distribution for the system can be built

Further author information: send correspondence to Stefano Beri: s.beri@lancaster.ac.uk or to Riccardo Mannella: mannella@df.unipi.it

up iteratively²³ performing the simulation in regions far away from the equilibrium states. In this way, the shift of singularities in the probability distribution, and oscillation of the probability at the boundary due to finite noise intensity, have been observed. These features are consistent with the predicted shift of optimal paths due to the finiteness of the noise intensity. However, simulations able to reveal the predicted shift in the optimal path with increasing noise intensity are still lacking: to address this question we need numerical approaches which yield, not the probability distributions, but rather the actual paths followed by the dynamics of the system of interest. Simulation techniques based on *dynamic importance sampling* (DIMS) were proposed²⁴ for 1-dimensional dynamical systems to study dynamics in the limit of very small noise intensity. DIMS aims to accelerate Monte Carlo integrations by adding an appropriately chosen biasing field to the equations of motion, which remain stochastic in nature. Standard techniques are then used to relate Monte Carlo results in the presence of the bias to the statistical observables of the original system.

The investigation of real systems (such as the lasers mentioned above) requires the analysis of higher dimensional nonequilibrium systems. However, the extension of DIMS to multidimensional systems is not straightforward. An earlier biasing technique,²⁵ introduced for both 1 and 2 dimensional systems, was found incapable of detecting either the shift of the escape path²² or saddle point avoidance,²⁶ both of which had been predicted theoretically. Moreover, in the presence of singularities, a bad choice of bias might hide important physical features of the system of interest. Note that other numerical approaches, like the umbrella sampling technique²⁷ are not appropriate for nonequilibrium systems.

The aim of this paper is the introduction of a generalized and robust version of DIMS valid, in principle for an arbitrary number of dimensions. Such an extended method would allow one to reveal the behaviour of the system in the vicinity of the MPEP in the finite noise regime. accelerating the simulation by exploitation of well-established zero-noise-limit theoretical results.

In order to give some concrete examples of the application of the technique, we apply it to the investigation of escape in three different multidimensional nonequilibrium systems: the inverted van der Pol oscillator, the harmonically driven overdamped Duffing oscillator and the polarization dynamics of a vertical cavity surface emitting laser. The noise intensities considered lie far beyond the range of anything investigated previously. As we will show, the predicted shift of the optimal path due to the finiteness of the noise is clearly resolved and turns out to be in excellent agreement with theory²² over more than 4 orders of magnitude in the noise intensity. The extension of the algorithm to stochastic maps is discussed.

2. THEORY

As mentioned in the introduction, stochastic nonlinear systems are used to describe a very large number of different physical problems. In order to keep the discussion as general as possible, we consider a generic nonlinear system under the influence of noise described by the following Langevin equation

$$\dot{x} = f(x) + \xi(t), \quad (1)$$

$$\langle \xi(t) \rangle = 0 \quad \langle \xi(t)\xi(s) \rangle = \epsilon\delta(t-s) \quad (2)$$

Here x represents a vector of coordinates, $f(x)$ is a nonlinear function, and $\xi(t)$ is a family of zero-mean uncorrelated Gaussian noise processes of intensity ϵ . The drift field $f(x)$ is chosen in order to display multiple stable states (including eventually $x \rightarrow \infty$) and noise induced transitions between them are considered. For systems in detailed balance (for example if $f(x)$ is the gradient of some potential function), activation takes place according to paths that are time-reversed relaxational trajectories.²⁸ In what follows, we consider the case where $f(x)$ does not satisfy the detailed balance condition, and we will focus on the important case of coexisting steady states whose basins of attraction are separated by saddle cycles.

The time evolution of the probability density for the system (1) is regulated by the following Fokker-Planck equation

$$\frac{\partial \rho}{\partial t} = -\frac{\partial (f\rho)}{\partial x} + \frac{\epsilon}{2} \frac{\partial^2 \rho}{\partial x^2} \quad (3)$$

In the limit $\epsilon \rightarrow 0$, (3) can be solved using the WKB expansion.^{13,14} The probability distribution is considered to have the form

$$\rho(x, t) = z(x, t) \exp\left(-\frac{S(x, t)}{\epsilon}\right), \quad \epsilon \rightarrow 0, \quad (4)$$

where $S(x, t)$ and $z(x, t)$ are two functions. Inserting (4) in (3) and considering different order of expansion in ϵ , at leading order ϵ^{-1} the auxiliary function S turns out to be the solution of the Hamilton-Jacobi equation for a classical action

$$\frac{\partial S}{\partial t} = -H\left(x, \frac{\partial S}{\partial x}\right). \quad (5)$$

The Hamiltonian for the system,

$$H(x, p) = \frac{p^2}{2} + p \cdot f, \quad (6)$$

is known as the Wentzell-Freidlin Hamiltonian¹⁴ and the Hamiltonian equations for the system are

$$\dot{x} = f(x) + p, \quad \dot{p} = -p \frac{df}{dx}. \quad (7)$$

The evolution of the function S along the solutions of (7) is calculated starting from $\frac{dS}{dt} = \frac{\partial S}{\partial t} + \frac{\partial S}{\partial x} \dot{x}$. Using $\frac{\partial S}{\partial x}$ together with Eq.(5) and Eq.(6), the final equation for the action is

$$\frac{dS}{dt} = \frac{1}{2} p^2. \quad (8)$$

Being non-decreasing along trajectories and differentiable almost everywhere, the function S can be considered as a non-equilibrium potential for the system.²⁹⁻³² It is known from the theory of dynamical systems that $S(x, t)$ can be a multi-valued function of position in the coordinate space.^{29,31,33,34} In this case, more than one trajectory solution of (5) reaches the same point in coordinate space. In the limit $\epsilon \rightarrow 0$, only that of least action S_{\min} is relevant, and all trajectories corresponding to higher values of S are exponentially disadvantaged. Escape takes place along the least action trajectory with overwhelming probability in the limit $\epsilon \rightarrow 0$. This is the MPEP, and the action calculated along it is the ‘‘activation energy’’. Regions of coordinate space reached by different families of optimal paths are separated by *switching lines* (SL).^{18,19,35} A trajectory ceases to be optimal after crossing a switching line. For this reason, the most probable escape path can touch the SL only asymptotically. Because the SL reaches the cycle asymptotically,¹⁸ the only possible optimal escape trajectories are heteroclinic paths connecting the initial state to the saddle cycle in infinite time.

To calculate the effect of finite, but small, $\epsilon \neq 0$ in this picture, a calculation of the next-to-leading order in the WKB expansion is performed. In this order of approximation, the *prefactor* $z(x, t)$ satisfies.¹⁹

$$\frac{dz}{dt} = -\frac{\partial f^i}{\partial x_i} z - \frac{1}{2} \frac{\partial^2 S}{\partial x_i \partial x_i} z \quad (9)$$

where summation over repeated indexes is understood. The solution of (9) calls for a knowledge of the second derivatives of the action calculated along the characteristics. Differentiating twice (5), the following equations are obtained¹⁹

$$\begin{aligned} \frac{d}{dt} \left(\frac{\partial^2 S}{\partial x^i \partial x^j} \right) &= -\frac{\partial^2 H}{\partial x^i \partial x^j} - \frac{\partial^2 S}{\partial x^i \partial x^k} \frac{\partial^2 H}{\partial p^k \partial x^j} \\ &\quad - \frac{\partial^2 S}{\partial x^j \partial x^l} \frac{\partial^2 H}{\partial x^i \partial p^l} - \frac{\partial^2 S}{\partial x^j \partial x^l} \frac{\partial^2 S}{\partial x^i \partial x^k} \frac{\partial^2 H}{\partial p^k \partial p^l} \end{aligned} \quad (10)$$

The non-constancy of the prefactor along the trajectories can be expressed in terms of a corrected non-equilibrium potential (dependent on ϵ)

$$S_\epsilon = S - \epsilon \log(z). \quad (11)$$

It is this corrected potential that has to be used to locate the position of the switching line for finite noise regimes. Points on the modified SL are defined by $S_\epsilon^1 = S_\epsilon^2$ where the index 1, 2 refers to two different trajectories reaching

the same point in the coordinate space.²³ The modified switching line does not touch the cycle asymptotically, but hits it at a definite position which depends on the noise intensity. As a consequence, heteroclinic trajectories are no longer optimal and the optimal escape follows a path that differs from the MPEP.

The case of a non-linear stochastic map is very similar. Consider a generic map of the form

$$x_{n+1} = f(x_n) + \xi_n, \quad (12)$$

$$\langle \xi_n \rangle = 0 \quad \langle \xi_n \xi_m \rangle = \epsilon \delta_{nm} \quad (13)$$

where the function $f(x)$ is chosen to display multiple coexisting stable states. As (12) is a discrete system, a Fokker-Plank equation cannot be written for the probability distribution. Nevertheless, it has been proved³⁶ that the MPEP for the map (12) satisfies the extended map

$$x_{n+1} = f(x_n) + \lambda_n, \quad (14)$$

$$\lambda_{n+1} = \left[\frac{\partial f}{\partial x} \Big|_{x_{n+1}} \right]^{-1T} \lambda_n. \quad (15)$$

Here the variable λ_n plays the role of the momentum p in (7) and the symbol T indicates the transpose matrix. The “action” for the solutions of (14) and (15) can be calculated using the discrete version of (8)

$$S_{n+1} = S_n + \frac{1}{2} \lambda_n^2 \quad (16)$$

In the same way as in continuous systems, the transitions from an initial stable state to a final state take place along the path that minimize (16).

3. ALGORITHM

In this section we propose we propose an extension of DIMS^{24,25} to the multidimensional case. It will be used to unravel features of the topology close to the optimal escape path in the limit of small but finite noise intensity. The method is applicable to continuous systems or maps characterized by a stable attractor with a sizable basin of attraction, where escape takes place via a large fluctuation.

Consider a generic dynamical system of the form (1); we will focus on the transitions from a stable attractor A_s toward a final saddle F_s . The process takes place in three steps: in the vicinity of A_s the dynamics of the stochastic system is purely diffusive; then, when the system leaves the vicinity of A_s (the length scale is defined by $\sqrt{\epsilon}$), the escape becomes essentially ballistic, along the MPEP and, in the vicinity of F_s , the finite noise diffusion dominates. In order to take into account the existence of these three regimes, the integration method is built as follow: the system is initially set close to A_s , the exact equations of motion (1) are integrated using a standard SDE (stochastic differential equation) integrator: for the examples shown below, we used the Heun integrator.³⁷ This reproduce the diffusive regime in the vicinity of A_s . We also set a boundary at some distance from the stable attractor: this boundary has nothing to do with the boundary of the basin of attraction, but it delineate where we define the diffusive regimes to change to ballistic. When the boundary is crossed, we switch from standard SDE integration to DIMS integration. Although the final result does not appear to depend on the boundary choice, nevertheless the boundary ought to be chosen on some rational basis: we require that the boundary should be fairly easily reached by the dynamical system when using straight SDE integration, but also that this event should not be too probable. In practice, a reasonable boundary could be e.g. a circle centered on the stable attractor, with a radius of a few $\sqrt{\epsilon}$. This choice reproduces the diffusive dynamics in the vicinity of the stable state. When the system hits the boundary, we switch to the DIMS integrator: from the above discussion, we know that the SDE

$$\dot{x} = f(x) + \xi(t)$$

maps onto the Hamiltonian equation (7), so we switch to the integration of

$$\dot{x} = f(x) + p(x) + \xi(t) \quad (17)$$

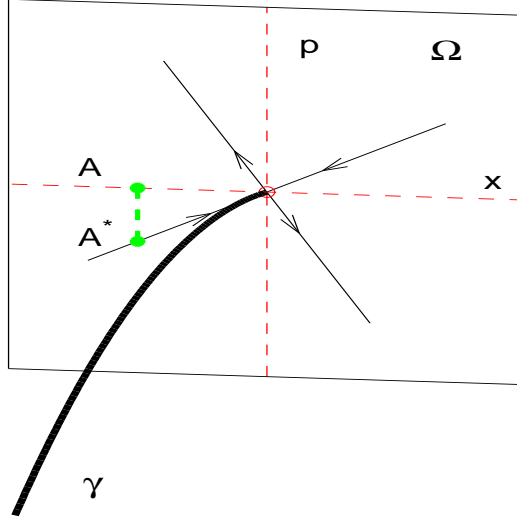


Figure 1. The scheme for one step of the DIMS method, where: Ω is a cross section in the extended phase space; γ (thick line) is the optimal path predicted by the theory; the thin lines are the stable and unstable eigenspaces (as indicated by the directions of the arrows) of the optimal path. The dashed lines represent respectively the coordinate space x and the momentum space p . A is a point in the coordinate space, A^* is the corresponding point on the stable manifold of γ as required by the integration procedure.

where $p(x)$ is the momentum conjugated with x as obtained from the MPEP and $\xi(t)$ is the DIMS stochastic component. It is clear that in more than one dimension the probability of being exactly on the MPEP during each integration time step is negligible: but the idea is that we should nevertheless use in the integration of (17) the value of $p(x)$ which “pulls” the escape tube toward the boundary. This is achieved by linearising the Hamilton equations near the MPEP, and using the $p(x)$ that keeps the system on the stable manifold of the MPEP. A step of the scheme is explained in Fig.1. Consider a point A in the coordinate space. The momentum $p(x)$ to be used in the equation (17) is calculated in the following way: the point A^* in the extended phase space which has the same x coordinate as A , and lies on the stable manifold of the MPEP, is located. The momentum of the point A^* is then used as $p(x)$ in (17). The integration scheme is interrupted and reset if the trajectory leaves a small neighborhood of the MPEP (size of a few $\sqrt{\epsilon}$). The generalization to stochastic maps is straightforward: once again it is necessary to define a boundary separating the diffusive region (in the vicinity of the initial stable state) and the ballistic region. Inside the diffusive region, Eq.(12) is integrated numerically in standard way; when the fluctuations bring the system in the ballistic region, the integration scheme switches to DIMS: instead of integrating directly Eq.(12), we integrate

$$x_{n+1} = f(x_n) + \lambda_n + \xi_n \quad (18)$$

where the “momentum” λ_n is chosen in order to “pull” the path toward the MPEP. If the trajectory leaves a neighborhood of the order of $\sqrt{\epsilon}$ from the MPEP, it is rejected and the integration is restarted from scratch.

4. EXAMPLES

In this section we show some explicit examples of the application of the multidimensional DIMS algorithm. First, we consider the inverted van der Pol oscillator (IVDP). It is characterized by the presence of an unstable cycle with a stable point at its centre. DIMS is used here to study transitions from the stable state to the limit cycle. The IVDP system is described by the following pair of equations

$$\begin{aligned} \dot{x} &= y \\ \dot{y} &= -x - 2\eta(1 - x^2)y + \sqrt{\epsilon}\xi(t) \end{aligned} \quad (19)$$

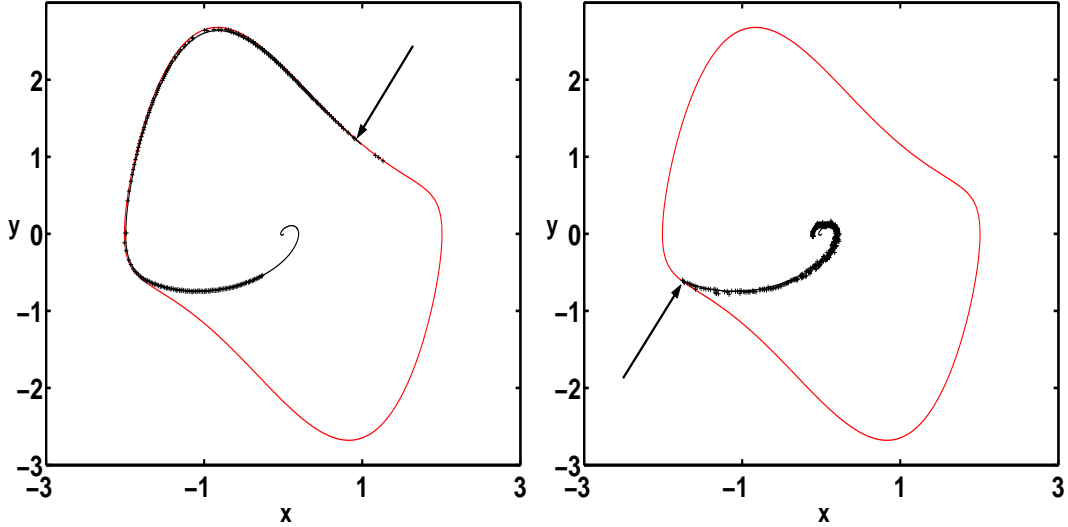


Figure 2. Comparison between theory and simulations for the escape in the IVDP system (19). Here the parameter $\eta = 0.5$ and two different noise intensities are considered: $\epsilon = 10^{-5}$ (left figure) and $\epsilon = 10^{-2}$ (right figure). The limit cycle and the most probable escape path are indicated by full lines; the crosses are points on the ridge of the prehistory probability density for the escape. The arrows indicate the positions where the theoretical modified optimal escape path hits the cycle. The theory agrees well with the experimental points for both noise intensities. A significant shift in the position where the optimal path hits the boundary is evident.

Here x and y are dynamical variables and $\xi(t)$ is a white Gaussian processes of unit intensity. The parameter η determines both the friction and the pumping of energy in the system. The DIMS simulations have been performed for a range of intensities running between 10^{-5} and 10^{-2} . Some results are shown in figure 2 for two different noise intensities. The agreement between the theoretical and experimental escape paths at finite noise intensities is seen to be excellent. The shift in the optimal path is continuous with the noise intensity and the change in the point where the MPEP hits the cycle is dramatic.

In order to show how the modified DIMS can be applied to non-autonomous stochastic systems we consider, as a second example, the harmonically driven overdamped Duffing oscillator

$$\dot{x} = x - x^3 + A \sin(\omega t) + \sqrt{\epsilon} \xi(t). \quad (20)$$

Here x is the dynamical coordinate, A and ω are the amplitude and the frequency of the external driving, and ξ is a white Gaussian process of unit intensity. The driving term $A \sin(\omega t)$ keeps the system out of equilibrium; the parameters A and ω are chosen to be in the non-perturbative, non-adiabatic regime. The dynamics of this system is characterized by two stable limit cycles separated by an unstable limit cycle. In the presence of noise, the system can fluctuate from one stable cycle to the other. Some simulation results are shown in Fig. 3. The experimental trajectory follows closely the heteroclinic path when it is far from the stable and unstable cycles. As the system approaches the unstable cycle, however, diffusion becomes important and the escape then runs along the finite noise escape path calculated using finite noise corrections. An increase in the noise intensity determines an increase in the shift of the hitting position of the experimental MPEP. Once again, the shift in the position is continuous with the noise intensity.

As a final example, we consider a noise-induced polarization switch in a VCSEL. If the linear dichroism of the active cavity and mirrors is small enough and the pumping is not too strong, the VCSEL emits in the fundamental transverse mode^{3,4,38} and the polarization switches between two orthogonally polarized modes. In this regime, the polarization dynamics can be described using the polarization angle ϕ and the ellipticity χ . The dynamical model for these is³

$$\dot{\chi} = \omega_l \sin(2\phi) - \gamma_n \sin(2\chi) \cos(2\chi) + \gamma_l \sin(2\chi) \cos(2\phi) + \xi_\chi(t) \quad (21)$$

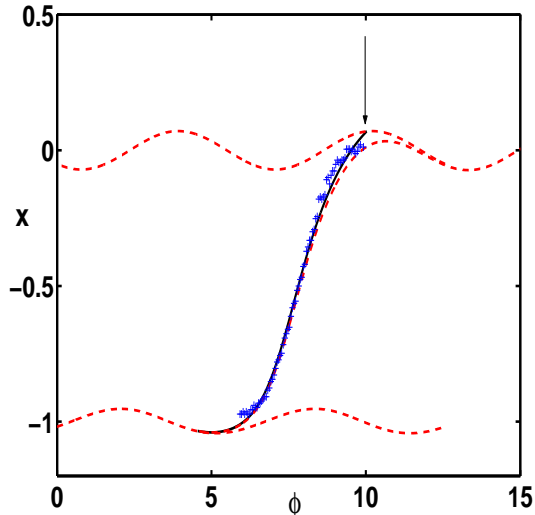


Figure 3. Comparison of theory and simulations for the activation problem in the Duffing system (20). The parameters are $A = 0.1$ and $\omega = 1$. The noise intensity is here $\epsilon = 4 \times 10^{-3}$. The dashed line indicate the steady states and the most probable escape path at $\epsilon = 0$. The solid line indicates the noise corrected optimal path. The crosses are points on the ridge of the prehistory probability density for the escape. The position where the noise corrected optimal path hits the saddle cycle is indicated by an arrow.

$$\dot{\phi} = -\omega_l \frac{\sin(2\chi)}{\cos(2\chi)} \cos(2\phi) + \gamma_l \frac{\sin(2\phi)}{\cos(2\chi)} - \omega_n \sin(2\chi) + \xi_\phi(t) \quad (22)$$

$$\langle \xi_\chi(t) \rangle = \langle \xi_\phi(t) \rangle = 0 \quad \forall t \quad (23)$$

$$\langle \xi_\chi(t) \xi_\chi(s) \rangle = \langle \xi_\phi(t) \xi_\phi(s) \rangle = \epsilon \delta(t-s) \quad \langle \xi_\phi(t) \xi_\chi(s) \rangle = 0 \quad \forall t, s \quad (24)$$

Here ω_l and γ_l are the dispersive (birefringence) and absorptive (dichroism) linear anisotropies, and γ_n and $\omega_n = \alpha \gamma_l$ (α is the linewidth enhancement factor) are the nonlinear anisotropies. The spontaneous emission of photons in the cavity is described by the Gaussian stochastic variables ξ_χ and ξ_ϕ . The dynamical variable χ may vary between $-\frac{\pi}{4}$ and $\frac{\pi}{4}$ and the angle ϕ may vary between 0 and π . With a proper choice of the parameters, two linear polarization modes are stable: the \hat{x} -polarized mode (corresponding to $\chi = 0$ and $\phi = 0$) and the \hat{y} -polarized mode (corresponding to $\chi = 0$ and $\phi = \frac{\pi}{2}$). Their basins of attractions are separated by an unstable limit cycle similar to the one in IVDP system.

The DIMS scheme has been applied here to investigate the transitions from the \hat{y} -polarized mode to the limit cycle. In figure 4 the numerical simulations are compared with the theoretical MPEP for different values of the noise intensity. As expected, when the noise intensity increases, the simulations follow the MPEP less closely and they leave the basin of attraction of the initial lasing mode earlier.

5. CONCLUSIONS AND DISCUSSION

In conclusion, in this paper we have introduced a way to perform numerical simulations in complex nonlinear systems that is efficient and robust. The main idea of the algorithm is to perform the simulation in the vicinity of the MPEP which can be calculated solving (7) for a continuous system or (14) and (15) for a stochastic map. The simulated trajectory is kept close to the MPEP taking the momentum so as to stay on the stable manifold. The method can be successfully applied to a large class of dynamical systems and maps. The technique is a very useful tool for the investigation of features induced by finite noise in the neighborhood of the optimal escape path; and hence leads to a biasing scheme that is based on the dynamics of the system itself, thus constituting a most natural scheme for dynamic importance sampling. The application of the method has allowed us to explore regimes of low but finite noise intensity, and enabled us to observe experimentally the predicted shift²³ of escape path; we stress that this shift is a large physical effect, even at the smallest noise intensities investigated

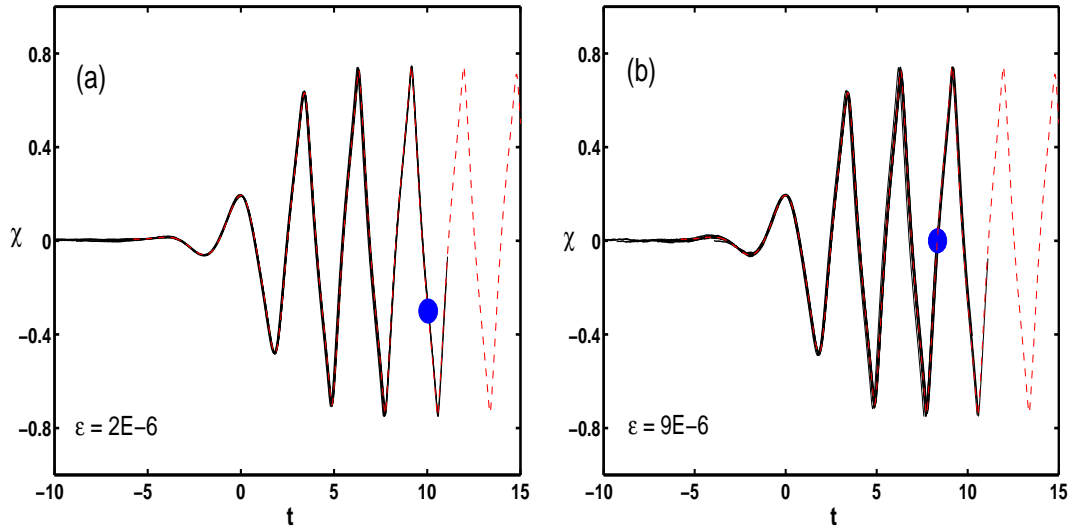


Figure 4. Comparison between theory and simulations for the polarization switches in a VCSEL. The noise intensity changes from (a) to (b); the dashed lines are the theoretical MPEP and the solid lines are the results of the simulation. The full circle marks the point where half of the trajectories plus one leave the basin of attraction of the initial lasing mode. The shift of this point with the noise intensity is evident.

in this paper. The technique provides a way of extending experimental studies to noise intensities that were previously inaccessible, and promises to accelerate research in many fields of science, e.g. in the investigation of the polarization of flip dynamics in vertical cavity surface emitting lasers or in the motion of ions in the pores of cellular membranes. The discrete version of the algorithm may be used as a tool to investigate problems in laser dynamics.^{39,40}

ACKNOWLEDGMENTS

We are grateful for valuable discussions with Dmitri Luchinsky and Stanislav Soskin. The research has been supported in part by the Engineering and Physical Sciences Research Council (UK) and by INTAS.

REFERENCES

1. M. B. Willemsen, M. P. van Exter, and J. Woerdman, "Anatomy of a polarization switch of a vertical-cavity semiconductor laser," *Phys. Rev. Lett.* **84**, pp. 43377–4340, 2000.
2. M. B. Willemsen, M. P. van Exter, and J. P. Woerdman, "Correlated fluctuations in the polarization modes of a vertical cavity semiconductor laser," *Phys. Rev. A* **60**, pp. 4105–4205, 1999.
3. M. P. van Exter, R. F. M. Hendriks, and J. P. Woerdman, "Physical insight into the polarization dynamics of semiconductor vertical-cavity lasers," *Phys. Rev. A* **57**, pp. 2080–2090, 1998.
4. M. P. van Exter, M. B. Willemsen, and J. P. Woerdman, "Polarization fluctuations in vertical-cavity semiconductor lasers," *Phys. Rev. A* **58**, pp. 4191–4205, 1998.
5. R. S. Eisenberg, M. M. Klosek, and Z. Schuss, "Diffusion as a chemical-reaction - stochastic trajectories between fixed concentrations," *J. Chem. Phys.* **102**, pp. 1767–1780, 1995.
6. M. I. Dykman, D. G. Luchinsky, R. Mannella, P. McClintock, N. D. Stein, and N. G. Stocks, "Stochastic resonance in perspective," *Nuovo Cimento D* **17**, pp. 661–683, 1995.
7. F. A. F. Julicher and J. Prost, "Modeling molecular motors," *Rev. Mod. Phys.* **69**, pp. 1269–1281, 1997.
8. M. O. Magnasco, "Forced thermal ratchets," *Phys. Rev. Lett.* **71**, pp. 1477–1481, 1993.
9. M. I. Dykman, H. Rabitz, V. N. Smelyanskiy, and B. E. Vugmeister, "Resonant directed diffusion in nonadiabatically driven systems," *Phys. Rev. Lett.* **79**, pp. 1178–1181, 1997.

10. H. Kramers, "Brownian motion in a field of force and the diffusion model of chemical reactions," *Physica* **7**, pp. 284–304, 1940.
11. V. I. Mel'nikov, "The Kramers problem: fifty years of development," *Phys. Rep.* **209**, pp. 1–71, 1991.
12. M. I. Dykman, "Large fluctuations and fluctuational transitions in systems driven by colored Gaussian noise—a high frequency noise," *Phys. Rev. A* **42**, pp. 2020–2029, 1990.
13. D. Ludwig, "Persistence of dynamical systems under random perturbations," *SIAM Rev.* **17**, pp. 605–640, 1975.
14. M. Freidlin and A. D. Wentzel, *Random Perturbations in Dynamical Systems*, Springer, New York, 1984.
15. R. S. Maier and D. L. Stein, "Effect of focusing and caustics on exit phenomena in systems lacking detailed balance," *Phys. Rev. Lett.* **71**, pp. 1783–1786, 1993.
16. R. S. Maier and D. L. Stein, "How an anomalous cusp bifurcates in a weak-noise system," *Phys. Rev. Lett.* **85**, pp. 1358–1361, 2000.
17. M. I. Dykman, M. M. Millonas, and V. N. Smelyanskiy, "Observable and hidden features of large fluctuations in nonequilibrium systems," *Phys. Lett. A* **195**, pp. 53–58, 1994.
18. V. N. Smelyanskiy and M. I. Dykman, "Topological features of large fluctuations to the interior of a limit cycle," *Phys. Rev. E* **55**, p. 2516, 1997.
19. R. S. Maier and D. L. Stein, "A scaling theory of bifurcations in the symmetrical weak-noise escape problem," *J. Stat. Phys.* **83**, pp. 291–357, 1996.
20. J. Lehmann, P. Reimann, and P. Hanggi, "Surmounting oscillating barriers: path-integral approach for weak noise," *Phys. Rev. E* **62**, pp. 1639–1642, 2000.
21. S. M. Soskin, V. I. Sheka, T. L. Linnik, and R. Mannella, "Short time scales in the Kramers problem: A stepwise growth of the escape flux," *Phys. Rev. Lett.* **86**, pp. 1665–1669, 2001.
22. A. Bandrivskyy, S. Beri, and D. G. Luchinsky, "Noise-induced shift of singularities in the pattern of optimal paths," *Phys. Lett. A* **314**, pp. 386–391, 2003.
23. A. Bandrivskyy, S. Beri, D. G. Luchinsky, R. Mannella, and P. McClintock, "Fast Monte Carlo simulations in the probability distributions of nonequilibrium systems," *Phys. Rev. Lett.* **90**, p. 210201, 2003.
24. D. M. Zuckermann and T. B. Woolf, "Efficient dynamic importance sampling of rare events in one dimension," *Phys. Rev. E* **63**, p. 016702, 2001.
25. T. B. Woolf, "Path corrected functionals of stochastic trajectories: towards relative free energy and reaction coordinate calculations," *Chem. Phys. Lett.* **289**, pp. 433–441, 1998.
26. D. G. Luchinsky, R. S. Maier, R. Mannella, P. V. E. McClintock, and D. L. Stein, "Observation of saddle-point avoidance in noise-induced escape," *Phys. Rev. Lett.* **82**, pp. 1806–1809, 1999.
27. C. Dellago, P. G. Bolhuis, F. S. Csajka, and D. Chandler, "Transition path sampling and the calculation of rate constants," *J. Chem. Phys.* **108**, pp. 1964–1977, 1998.
28. D. G. Luchinsky and P. V. E. McClintock, "Irreversibility of classical fluctuations studied in analogue electrical circuits," *Nature* **389**, pp. 463–466, 1997.
29. R. Graham and T. Tel, "Existence of a potential for dissipative dynamical systems," *Phys. Rev. Lett.* **52**, pp. 9–12, 1984.
30. R. Graham and T. Tel, "Weak noise limit of fokker-planck models and nondifferentiable potentials for dissipative dynamical systems," *Phys. Rev. A* **31**, pp. 1109–1122, 1985.
31. H. R. Jauslin, "Nondifferentiable potentials for nonequilibrium steady states," *Physica A* **144**, pp. 179–191, 1987.
32. R. Graham, "Macroscopic potentials, bifurcation and noise in dissipative systems," in *Noise in Nonlinear Dynamical Systems*, F. Moss and P. V. E. McClintock, eds., **1**, pp. 225–278, Cambridge University Press, 1989.
33. V. Arnold, *Mathematical Methods of Classical Mechanics*, Springer-Verlag, Berlin, 1978.
34. M. V. Day, "Recent progress on the small parameter exit problem," *Stochastics* **20**, pp. 121–150, 1987.
35. M. I. Dykman, P. V. McClintock, V. N. Smelyanskiy, N. D. Stein, and N. G. Stocks, "Optimal paths and the prehistory problem for large fluctuations in noise driven systems," *Phys. Rev. Lett.* **68**(18), pp. 2718–2721, 1992.
36. P. Grassberger, "Noise induced escape from attractors," *Phys. A* **22**, pp. 3283–3290, 1989.

37. R. Mannella, "Integration of stochastic differential equations on a computer," *Int. J. Mod. Phys C* **13**, pp. 1177–1194, 2002.
38. M. P. van Exter, A. Al-Remawi, and J. P. Woerdman, "Polarization fluctuations demonstrate nonlinear anisotropy of a vertical-cavity semiconductor laser," *Phys. Rev. Lett.* **80**, pp. 4875–4878, 1998.
39. V. A. Gaisyonok, E. V. Grigorieva, and S. A. Kashchenko, "Poincaré mappings for targeting orbits in periodically driven lasers," *Opt. Commun.* **124**, pp. 408–417, 1996.
40. V. Chizhevsky, E. V. Grigorieva, and S. A. Kashchenko, "Optimal timing for targeting periodic orbits in a loss-driven CO₂ laser," *Opt. Commun.* **133**, pp. 189–195, 1997.